JOURNAL OF GUIDANCE, CONTROL, AND DYNAMICS
Vol. 20, No. 5, September–October 1997

Optimal Mass Flexible Tethers for Aerobraking Maneuvers

Jordi Puig-Suari*
Arizona State University, Tempe, Arizona 85287-6106

Previous results using a rigid tether model indicate that tether mass in aerobraking maneuvers is much lower than the propellant mass required for a similar maneuver. In this work the effects of flexibility on the optimum maneuvers are studied. The results indicate that tether flexibility produces a small increase in tether mass but it remains significantly lower than propellant mass. The effects of flexibility are greater in maneuvers where the tether remains nearly vertical during flythrough. However, bending on the tether in the optimum maneuvers is small and the tether aerobraking maneuver remains feasible when tether flexibility is included in the analysis.

I. Introduction

MANY applications of tethers in the atmosphere have been proposed, and much work has been presented on the subject.[1–12] However, some of the most popular applications, such as upper atmosphere research, do not use aerodynamic forces to actively maneuver the spacecraft. Work on aeromaneuvering with tethers is limited but includes applications such as re-entry problems[3] and the use of lifting bodies to stabilize tethered systems in the atmosphere.[4]

One of the more demanding atmospheric applications proposed for tethered satellites is the aerobraking tether. This idea was first published by Carroll[7] in 1986, but no analysis was done. The concept is ideally suited to dual vehicle missions consisting of an orbiter and a probe, which is delivered to the planet's surface or atmosphere, e.g., Galileo and Cassini. The two spacecraft are connected with a long tether, and on arrival to the target planet, the probe flies through the atmosphere while the orbiter remains high above the significant atmosphere and requires no heat shielding (see Fig. 1). Aerodynamic forces on the probe and the tether decelerate the system into a capture orbit about the planet. After the maneuver, the tether can be severed, placing the probe into a re-entry trajectory, or the system can remain together and perform additional maneuvers.

II. Rigid Tether Results

The feasibility of aerobraking tethers was first determined by Puig-Suari and Longuski.[8] In this analysis a rigid rod tether model is used. The model includes the following simplifying assumptions. The motion of the system is constrained to the orbit plane. The spacecraft (orbiter and probe) are analyzed as particles. Gravitational forces on the system are modeled using an inverse square law ($F_g = \mu m/R^2$). Because the rod is assumed to be massive, gravitational forces are integrated along the tether. Aerodynamic forces are calculated assuming a velocity-squared drag law

$$F_d = \tfrac{1}{2}\rho C_D S V^2 \tag{1}$$

where C_D is the drag coefficient, S is the frontal area, V is the wind velocity, and ρ is the atmospheric density, which is assumed to follow an exponential profile

$$\rho_i = \rho_0 \exp[(h_0 - h_i)/H] \tag{2}$$

where ρ_i is the atmospheric density at altitude h_i, ρ_0 is the reference density at altitude h_0, and H is the scale height. Again, aerodynamic forces on the tether are integrated along its length. A detailed derivation of the equations of motion for the system can be found in Ref. 8. Initial work on the aerobraking tether[9] concentrates on the vertical dumbbell maneuver, where the tether is in a vertical orientation ($\alpha_{\min} \cong 0$) during closest approach (see Fig. 1). This maneuver is chosen initially to obtain a large altitude difference (clearance) between the orbiter and the probe. However, moments due to the large aerodynamic forces acting on the probe and the lower section of the tether tend to rotate the system and plunge the orbiter into the atmosphere. This effect can be eliminated by spinning the system in the opposite direction before atmospheric impact (Ω_{in}) (Ref. 9). In this analysis the system is designed to minimize the normal forces on the rigid tether model. It is assumed that normal forces in the rigid model translate into bending when a more realistic flexible tether is used. The reduction of the normal forces at the tether attachment points can be accomplished by meeting the following two matching conditions.

1) Center matching is defined as follows. If the aerodynamic forces during flythrough are considered approximately impulsive (results indicate that, in aerocapture maneuvers, most aerodynamic effects occur in a short time interval around periapsis), normal forces at the orbiter attachment point are minimized when the aerodynamic forces on the system act at the center of percussion of the tether system about the orbiter. That is, when the center of pressure of the aerodynamic forces and the center of percussion about the orbiter are located at the same point on the tether.

2) Aeromatching is defined as follows. Normal forces at the probe attachment are minimized when the ballistic coefficients of the probe and the tether are approximately equal. When this is accomplished, the aerodynamic decelerations of the probe and the end of the tether are the same and shear forces at the attachment point are eliminated. Because of the low density of the tether materials, very large probe areas are required to satisfy this condition.

Using matched tethered systems, i.e., systems that meet the two just-defined matching conditions, vertical dumbbell aerobraking maneuvers at all of the atmosphere-bearing planets in the solar system and Titan are presented in Ref. 9. Maneuvers are designed to capture the system into a near parabolic orbit ($e = 0.9999$), with the incoming hyperbolic trajectories representing Hohmann transfers from Earth. The orbiter and the probe each have a mass of 1000 kg. The tether is assumed to be made of graphite with an ultimate strength of 3.6 GN/m^2 and a density of 1800 kg/m^3, and the target clearance Δh_t is approximately 1.8 times the scale height of the planet's atmosphere. In every case the mass of the tether is lower than the propellant mass required to capture the orbiter (the probe is assumed to use aerobraking to achieve capture as in the Galileo mission). Note that in this calculation an I_{sp} of 300 s is assumed for the propellant. These results are very encouraging, but the study is limited to vertical dumbbell maneuvers.

In Ref. 10 the analysis is extended with the development of optimization tools to determine the maneuver that requires the minimum tether mass. The basic problem is to obtain initial conditions for the tether trajectory and tether dimensions that minimize the mass of the tether while producing an acceptable maneuver. The trajectory is determined by the initial tether orientation and spin rate, α_0 and $\dot{\alpha}_0$, outside the atmosphere and the periapsis radius R_p of the inbound hyperbolic orbit. The tether is completely defined by its length l, and once it is established, the tether diameter is iteratively computed so

Received July 10, 1995; revision received April 18, 1997; accepted for publication April 18, 1997.

*Assistant Professor, Department of Mechanical and Aerospace Engineering. Member AIAA.

Table 1 Optimum maneuvers for rigid tether model (e_t = 0.9999, graphite tether, propellant I_{sp} = 300 s)

Maneuver	ΔV, km/s	Propellant mass, kg	Probe area, m^2	Δh_t, km	Length, km	Diameter, mm	Mass, kg	$\dot{\alpha}_0$, rad/s	R_p, km	$\alpha_{\min}$, deg
Mars (matched)	0.67	256	560	12.4	19.0	1.52	62.2	1.74*e*-2	3,484	49.2
Mars (unmatched)	0.67	256	100	12.4	18.6	1.49	58.4	1.66*e*-2	3,471	48.3
Jupiter (matched)	0.27	96	2,400	36.1	36.4	0.605	18.9	8.06*e*-3	71,877	−0.23
Jupiter (unmatched)	0.27	96	500	36.1	38.3	0.587	18.7	7.47*e*-3	71,848	3.30

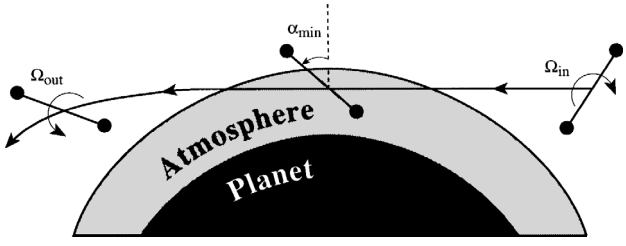

Fig. 1 Tether aerobraking maneuver.

that the tether withstands the forces produced by the maneuver. The constraints that determine an acceptable trajectory are as follows: the final eccentricity of the trajectory must equal the target eccentricity ($e = e_t$), the orbiter clearance over the probe must be greater than a minimum target clearance ($\Delta h > \Delta h_t$), and the tension forces must always be positive (compression is not acceptable in a tethered system). This can be written mathematically as a parameter optimization problem with equality and inequality constraints.[10]

Minimize:

$$F_{\max}(x) \qquad x = [\alpha_0, \dot{\alpha}_0, R_p, l] \tag{3}$$

Subject to:

$$e - e_t = 0 \tag{4}$$

$$\Delta h - \Delta h_t > 0 \tag{5}$$

$$T_{\min} > 0 \tag{6}$$

The problem can then be solved using nonlinear programming methods. In Ref. 10 the optimization is performed using an exterior penalty method using Powell's method for the unconstrained minimizations and a golden section method for the one-dimensional minimizations. Note, however, that the evaluation of the objective function in this problem, i.e., tether mass, requires the numerical simulation of a complete tether aerocapture maneuver, which makes the analysis very demanding computationally. For this reason, the rigid rod model is used (in lieu of a flexible model) for the simulations in Ref. 10. Numerical techniques do not guarantee that the result is optimum, only that it is a local minimum. However, graphical optimization techniques developed in Ref. 11 confirm the optimality of the solutions. The optimal results represent a significant improvement in tether mass. In addition, they indicate that the vertical dumbbell maneuver is not always the best solution, and a second maneuver emerges as optimal in some cases. In this new maneuver, the tether has an inclined orientation at closest approach ($\alpha_{\min} > 0$). Again, the analysis in Ref. 10 includes missions to all of the planets. Note that in Ref. 10 large probe areas are included in the systems, which results in nearly matched tether systems. The previous results are very encouraging and indicate that aerobraking tethers may provide an interesting alternative to propulsive maneuvers.[8–10] However, two issues remain to be addressed: the use of smaller (more realistic) probe areas, which result in tether systems that violate the two matching conditions, i.e., unmatched tether systems, and the effects of tether flexibility on the aerobraking maneuvers. These issues are studied using aerobraking maneuvers at Jupiter and Mars as examples of vertical dumbbell and inclined solutions, respectively.

The first step is to use the rigid rod model to find optimum aerobraking maneuvers for matched and unmatched tether systems at Mars and Jupiter. The maneuvers are based on those found in Refs. 9 and 10 (orbiter and probe mass of 1000 kg, graphite tethers, arrival trajectory based on a Hohmann transfers from Earth, and capture into near parabolic orbit). The main characteristics of these optimum solutions are shown in Table 1. As would be expected, the unmatched systems with the smaller probe areas require a lower periapsis radius to achieve capture. Otherwise, the only significant difference between the matched and unmatched systems is a small reduction in tether mass for the Mars unmatched system. To better understand the dynamics of these maneuvers, they are simulated using the rigid rod model (the same model used in the optimization).

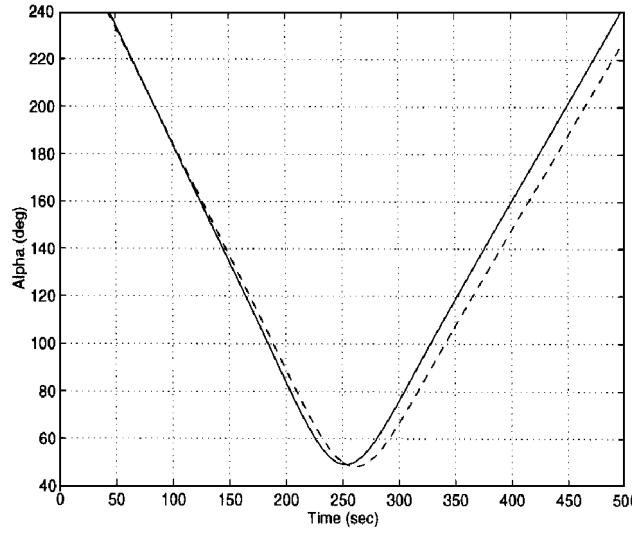

Fig. 2 Tether angle; rigid simulation of Mars rigid optimum: ——, matched and – – –, unmatched.

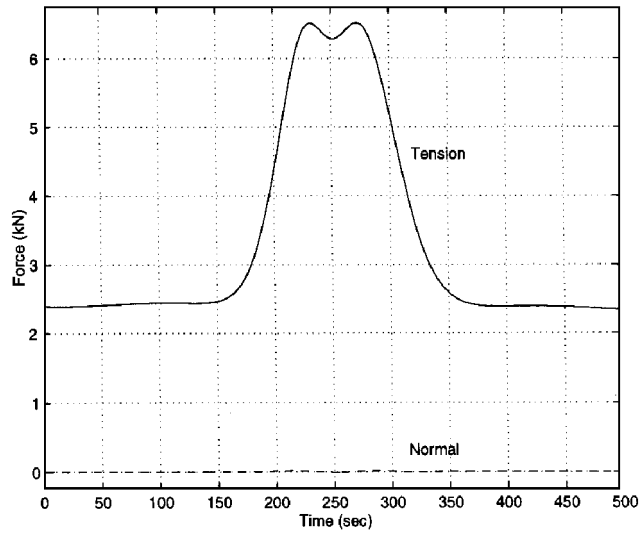

Fig. 3 Tether forces on the probe and the orbiter; rigid simulation of Mars rigid optimum, matched.

The simulation results for the optimum maneuvers at Mars are shown in Figs. 2–4. For both Mars systems, the optimum maneuvers are inclined maneuvers, $\alpha_{\min} \cong 50$ deg, with very similar changes in orientation, as can be seen in the angle plot (Fig. 2). As expected from inclined-type maneuvers, in both systems the maximum

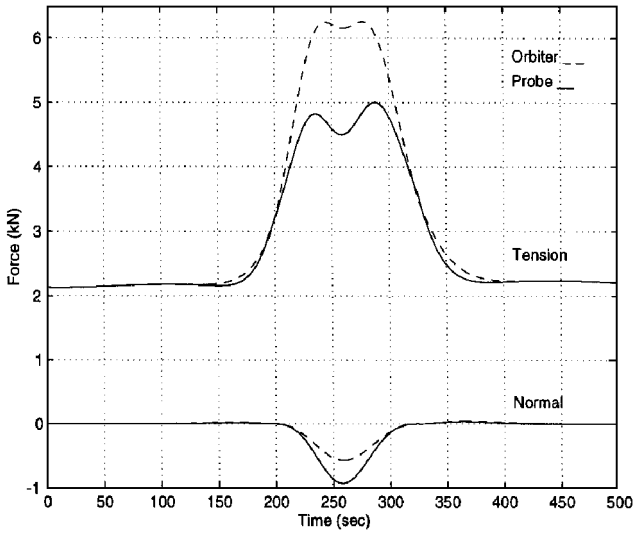

Fig. 4 Tether forces on the probe and the orbiter; rigid simulation of Mars rigid optimum, unmatched.

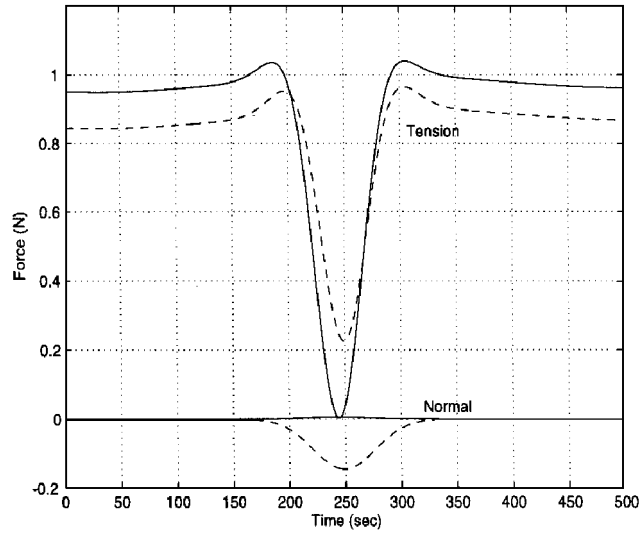

Fig. 6 Tether forces on the probe; rigid simulation of Jupiter rigid optimum: ——, matched and – – –, unmatched.

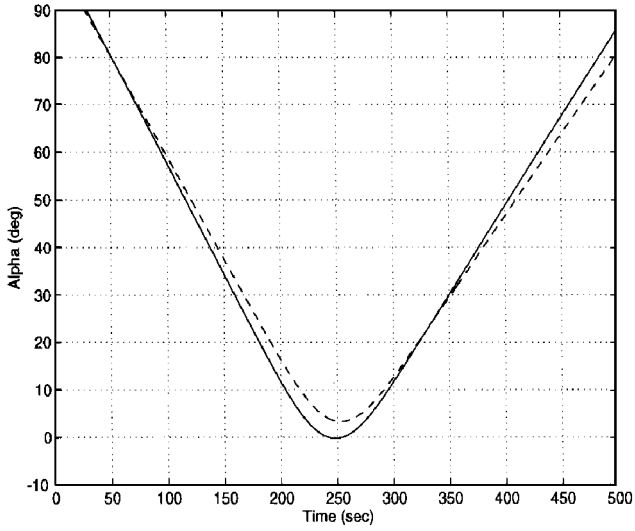

Fig. 5 Tether angle; rigid simulation of Jupiter rigid optimum: ——, matched and – – –, unmatched.

tension occurs during flythrough (150–350 s), where a large component of the aerodynamic forces acts along the tether (Figs. 3 and 4). Lower tension forces caused by the spin rate of the system are present before and after atmospheric flythrough. The tension plots show significant differences between the matched and unmatched systems. First, in the matched case, tension forces at the orbiter and probe ends of the tether are indistinguishable. This is because almost all of the aerodynamic effects are produced by the probe. On the other hand, for the unmatched system, the forces on the orbiter end are much larger than those at the probe. This is because the smaller probe requires a lower flythrough altitude and aerodynamic forces on the tether play an important role in decelerating the system. In addition, the aerodynamic forces on the orbiter, while still small, produce some deceleration on the orbiter and are responsible for the slight decrease in maximum forces on the tether. This explains why the tether mass in the Mars case is smaller in the unmatched system than in the matched one. Second, as expected, significant normal forces occur during flythrough in the unmatched system. However, in an inclined maneuver, this is the point where tension forces, i.e., tether stiffness, are at a maximum; thus, bending is expected to be small when a flexible tether is used.

The simulation results for the optimum solutions at Jupiter are shown in Figs. 5 and 6. The angle plot (Fig. 5) indicates that the matched system displays the basic characteristics of a dumbbell maneuver, with nearly vertical orientation at closest approach ($\alpha_{\min} \cong 0$), whereas the unmatched system is close to a vertical dumbbell but $\alpha_{\min}$ is slightly larger than zero. This difference has a significant effect on the tension on the system. In a vertical dumbbell maneuver, the forces on the tether are caused mostly by the tether spin before and after atmospheric flythrough, and they become nearly zero during flythrough when the system stops spinning and the aerodynamic forces are acting perpendicular to the tether ($\alpha_{\min} \cong 0$). This is clearly the behavior of the matched system (Fig. 6). For the unmatched system, some tension remains on the system at closest approach due to the nonzero value of $\alpha_{\min}$. Note that only forces on the probe are displayed in Fig. 6 because those on the orbiter are nearly identical for both Jupiter maneuvers. Again, this is because almost all aerodynamic forces are produced by the large probes. Also, as expected, normal forces are close to zero for the matched system but are significant in the unmatched case. Note that, in the dumbbell-type maneuvers, normal forces occur at the point on the trajectory where the tension is at its lowest, that is, where the stiffness of the tether is at a minimum. In a flexible tether, this effect may produce significant bending.[12]

Note that, in all of the maneuvers, the tension forces due to spin are approximately equal before and after the flythrough maneuver. This spin-matching condition,[9] where the spin rates of the tether before and after the maneuver (Ω_{in} and Ω_{out} in Fig. 1) have the same magnitude, has been found to be a characteristic of many optimum maneuvers developed using the rigid rod tether model.

Next, tether flexibility must be included in the analysis to determine the success of these tether aerobraking maneuvers.

III. Flexibility Effects on the Optimum Maneuvers

A. Flexible Model

The flexible tether model (Fig. 7) developed in Ref. 12 is used to study the effects of flexibility on the aerobraking tether system. The main assumptions and features of this model are the following (for the complete equations of motion for the system, see Ref. 12). The end masses are treated as particles because their dimensions are much smaller than those of the complete system. The motion of the system is constrained to the plane of the orbit. This is a common assumption because out-of-plane effects are usually small. The flexible tether is modeled as a collection of massive hinged rigid rods (Fig. 7). The number of rods and the length of each rod are arbitrary, so that the flexible effects can be modeled to an arbitrary level of accuracy. The gravity effects are integrated over each rod using an inverse square gravity model. Similarly, aerodynamic forces are integrated over the length of each rod, assuming a velocity-squared drag law with an exponential atmospheric density profile as defined in Eqs. (1) and (2). The main advantage of the rod model over traditional bead models is the ability to accurately model the aerodynamic effects with a small number of elements, thus reducing the numerical complexity of the problem. This is especially important in problems such as aerobraking where aerodynamic forces are

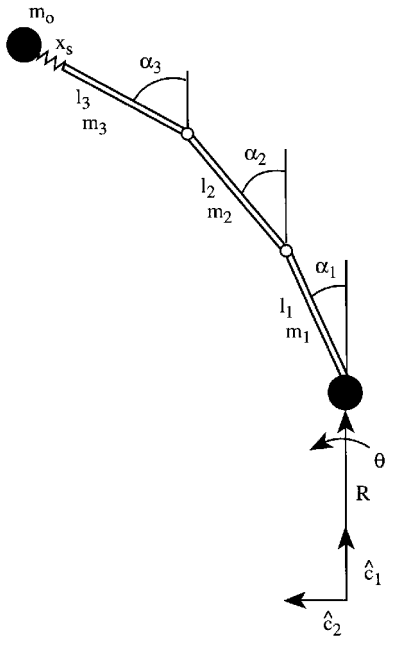

Fig. 7 Flexible tether model.

significant. In addition, to simulate the tether stretching during the maneuver, a spring is included at the connection between the orbiter and the tether, with a spring constant K_s given by

$$K_s = EA/l_t \tag{7}$$

where A and E are the cross-sectional area and tensile module of the tether, respectively. For the graphite used here, $E = 240$ GN/m^2. The flexible model also allows for the inclusion of a damper, i.e., a shock absorber, at the orbiter attachment point. The results in Ref. 12 are limited to nonoptimum vertical dumbbell maneuvers but indicate that the damping significantly reduces tether forces on flexible tethers performing aerobraking maneuvers. In this analysis, the damping coefficient C is set to

$$C = 2\sqrt{\frac{K_s m_o m_p}{m_o + m_p}} \tag{8}$$

where m_o and m_p are the masses of the orbiter and the probe, respectively. This damping ratio approximates a critically damped system. (Recall that the results presented here assume $m_o = m_p = 1000$ kg.) Note that thin tethers have very little bending resistance; hence, no torsional springs are included at the hinges.

In the flexible simulations, the spring is assumed to be unstretched initially. This makes the problem much easier when the flexible model is used in the optimization process. Because of the large damping present in the system, the longitudinal oscillations disappear before the system reaches the atmosphere and do not affect the flythrough maneuver (this can be clearly seen in the tension plots). In addition, the flexible tethers are modeled using only three segments. This is sufficient to obtain an approximation of the flexible behavior of the tether, while reducing the computational requirements to an acceptable level for numerical optimization. Recall that, with the hinged rod model, aerodynamic effects are accurately modeled with a small number of tether elements.

Next, the flexible model is used to simulate the optimum maneuvers obtained using the rigid rod model (Table 1).

B. Inclined Case (Mars)

Results from the three-rod flexible simulation of the tether system and maneuver for the matched tether at Mars (Table 1) are shown in Figs. 8 and 9. Again, Fig. 8 shows only the tether forces on the probe because forces on the orbiter are nearly equal. The basic characteristics of the maneuver are similar to those in the rigid simulation. Yet, there are two important differences. 1) Tension on the tether increases slightly, which would cause the tether designed using the rigid rod model to break. 2) Stretching in the tether changes the flythrough altitude of the probe, producing small changes in the final

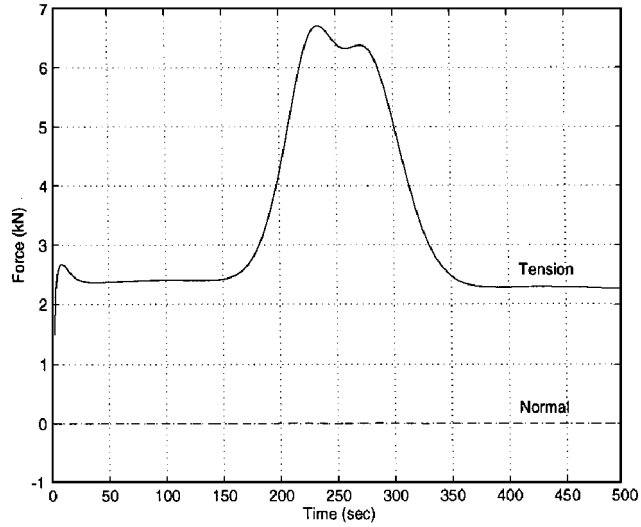

Fig. 8 Tether forces on the probe; flexible simulation of Mars rigid optimum, matched.

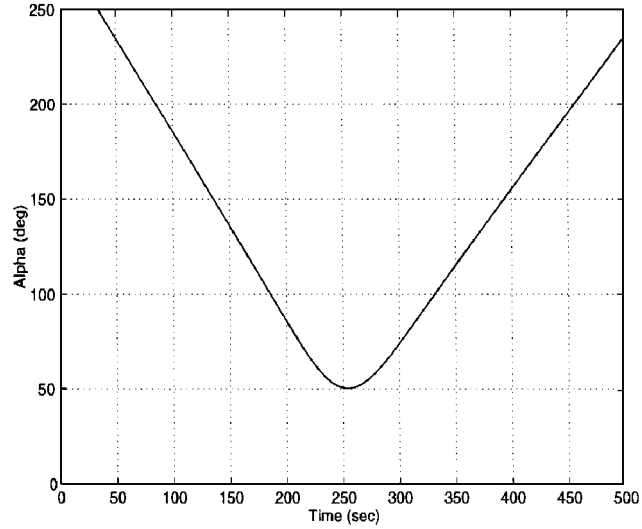

Fig. 9 Tether angles; flexible simulation of Mars rigid optimum, matched.

eccentricity. Note, however, that there is very little bending on the tether, as can be clearly seen in Fig. 9, where the α plots for the three rods are indistinguishable. Moreover, the tether orientation history and $\alpha_{\min}$ are very close to those in the rigid case.

For the unmatched tether, the flexible results are shown in Figs. 10 and 11. Here the results display greater differences from the rigid case, although the basic characteristics are quite similar. As in the matched case, the tension is slightly larger in the flexible case, which again would break the tether. Note that some normal forces remain because only three rods were used in the simulations. The α plots clearly show tether bending during atmospheric flythrough, as was predicted from the presence of normal forces in the rigid case. However, the bending is not severe and disappears after atmospheric passage, but it does have an effect in the trajectory because it changes the probe altitude, thus slightly changing the final eccentricity of the system.

Overall, the flexible simulations of the inclined optimum maneuvers obtained for aerocapture at Mars are very encouraging, indicating that the effects of flexibility on the system are benign and only small changes in the trajectory and the tether design are required.

C. Vertical Dumbbell Case (Jupiter)

The results of simulating the vertical dumbbell optimum maneuvers in Table 1 with the flexible model show radical differences

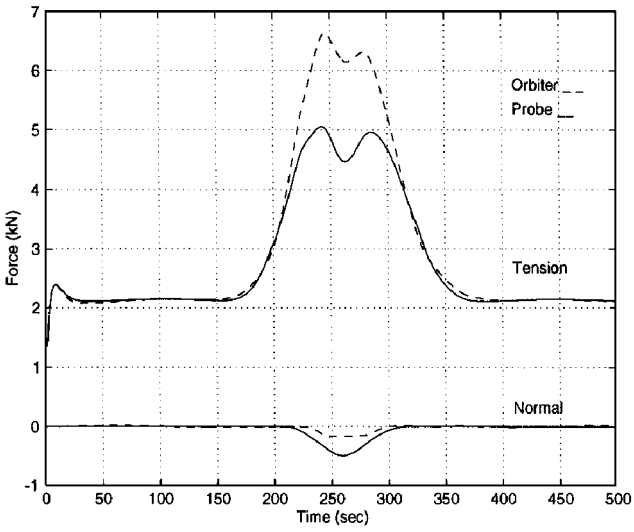

Fig. 10 Tether forces on the probe and the orbiter; flexible simulation of Mars rigid optimum, unmatched.

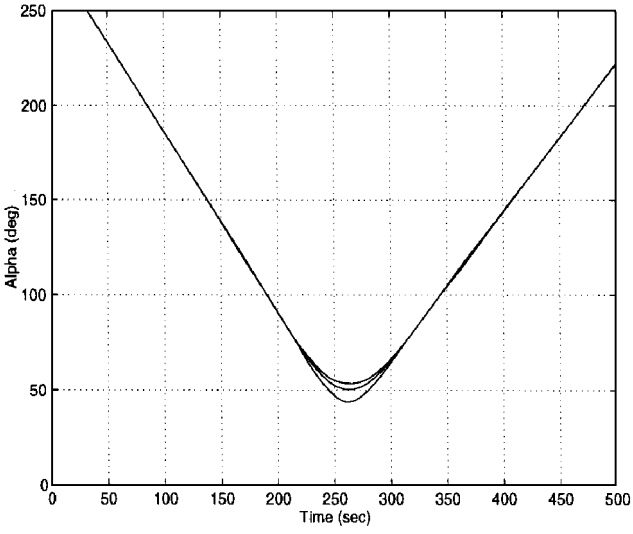

Fig. 11 Tether angles; flexible simulation of Mars rigid optimum, unmatched.

with the rigid results. First, the matched tether system is shown in Figs. 12 and 13. As in the inclined maneuver, the tension forces in the flexible simulation are larger than those in the rigid case. However, the biggest difference is the presence of large normal forces at the orbiter. Note that at the probe the normal forces are much smaller. It is unclear at this point why this behavior occurs. It could be produced by the presence of the spring at the orbiter attachment point, but the lack of normal forces in the inclined maneuver is not consistent with this explanation and further analysis is required. During atmospheric flythrough, a small amount of bending is present in the tether (recall that this system is matched). Very small bending oscillations remain after the maneuver. This behavior is quite different from the inclined solution where, even for the unmatched system, no bending is present after flythrough. As in the Mars case, the final eccentricity is changed slightly due to the effects of tether stretching and bending during the probe's flythrough trajectory.

Next, the results for the unmatched system (Figs. 14 and 15) show even greater flexible effects. As expected from the rigid results, the bending on the tether is quite large in this case. This produces a very large increase (over 100%) in the forces on the tether. In addition, as in the matched case, normal forces at the orbiter are much larger than those at the probe. Again, the desired final eccentricity is not achieved due to the changes on the probe trajectory.

These results indicate that tether flexibility has a significant effect on the vertical dumbbell maneuvers (much more than on the inclined

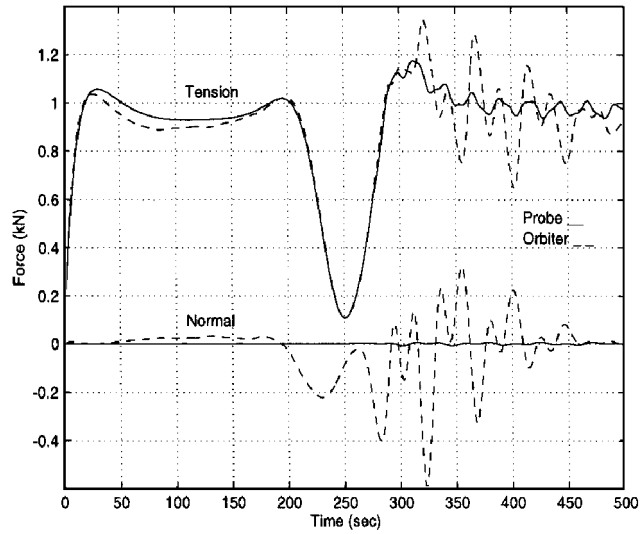

Fig. 12 Tether forces on the probe and the orbiter; flexible simulation of Jupiter rigid optimum, matched.

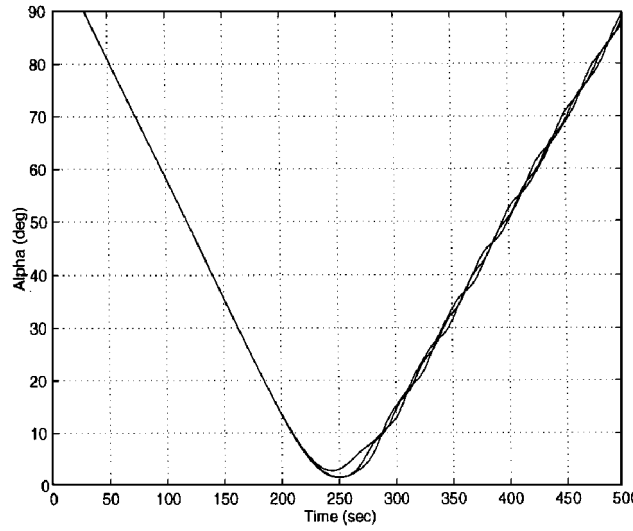

Fig. 13 Tether angles; flexible simulation of Jupiter rigid optimum, matched.

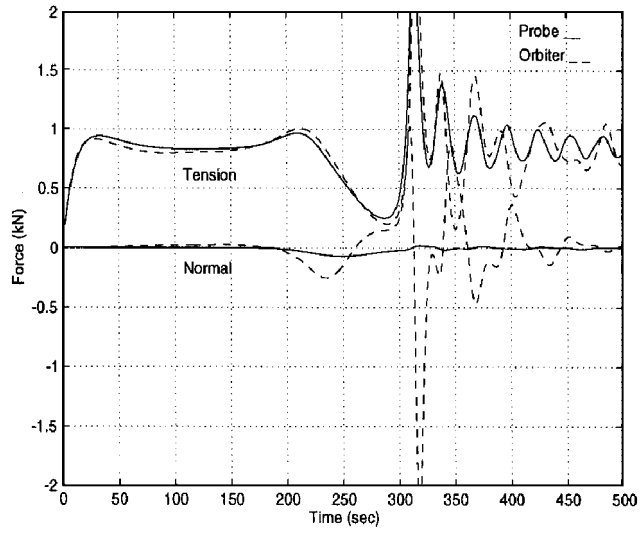

Fig. 14 Tether forces on the probe and the orbiter; flexible simulation of Jupiter rigid optimum, unmatched.

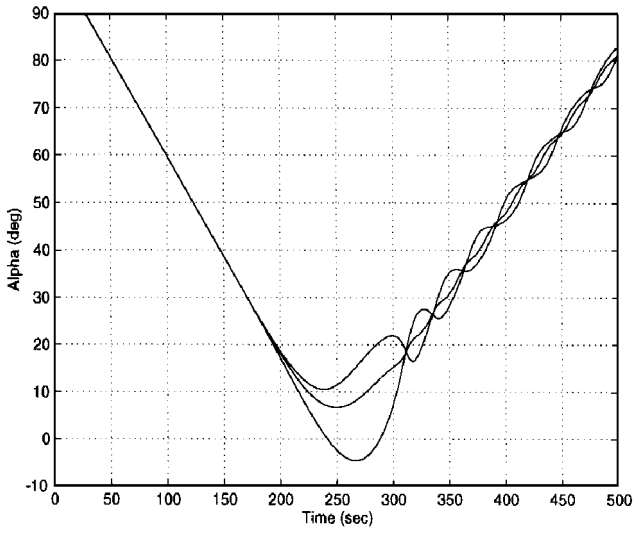

Fig. 15 Tether angles; flexible simulation of Jupiter rigid optimum, unmatched.

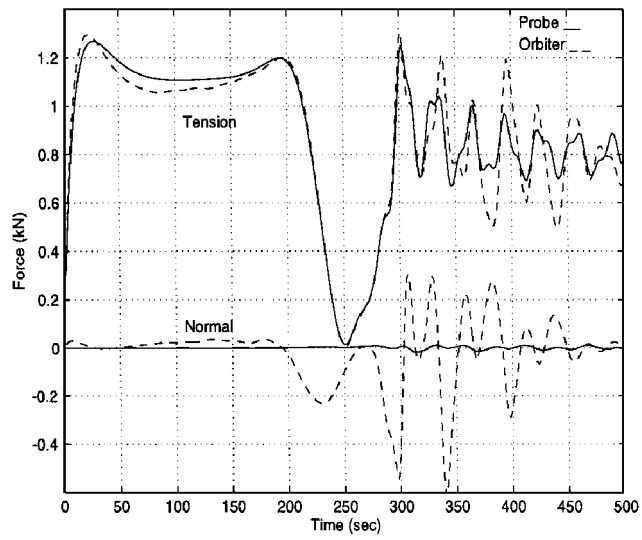

Fig. 16 Tether forces on the probe and the orbiter; flexible simulation of Jupiter flexible optimum, matched.

maneuvers). Consequently, significant changes to the system are required to obtain an acceptable maneuver. In addition, unmatching the tether in dumbbell maneuvers produces catastrophic behavior, making this maneuver type more sensitive to uncertainties.

Overall, the flexible results indicate that the optimum maneuvers obtained using the rigid model are not entirely acceptable. (Tether strength is too small in all cases, final eccentricity changes slightly, and catastrophic behavior occurs in some maneuvers.) Therefore, the optimization process should be improved by incorporating tether flexibility.

IV. Flexible Tether Optimization

The optimization tools previously developed[10] can be modified to use the flexible tether model when determining the tether mass corresponding to a set of initial conditions and tether dimensions. As mentioned earlier, to ease the computational process the flexible tether is modeled using only three rods. Note that the flexible model can incorporate an arbitrary number of rods, and, if computer power is not an issue, tether flexibility can be modeled to an arbitrary level of accuracy. The basic characteristics of the optimum flexible maneuvers are given in Table 2.

A. Inclined Case (Mars)

For the inclined maneuvers at Mars, the optimum maneuvers for the flexible tether model are very similar to those obtained with the rigid rod model. For both probe areas, the tension and α plots are nearly identical to those in Figs. 8–11 and so are not shown here. The only significant change is an increase in tether mass to withstand the larger forces that occur in the flexible system. Even with these changes, it is clear that in this maneuver the results obtained with the rigid rod model provide a very good approximation to the characteristics of the optimum tether. An accurate approximation to the mass of the optimum flexible solution can be obtained by increasing the tether diameter so that it can withstand the forces observed in the flexible simulation. Note that the mass increase is slightly larger in the unmatched system where bending occurs.

B. Vertical Dumbbell Case (Jupiter)

The flexible optimization is much more interesting in the vertical dumbbell maneuvers at Jupiter because the effects of flexibility on the rigid rod solution are very significant. The results from the simulations of the optimum maneuvers obtained with the flexible model are shown in Figs. 16–19. For the matched system (Figs. 16 and 17), the behavior of the flexible optimal solution is very similar to that of the rigid solution. However, there is a noticeable increase in the initial spin rate, which produces a vertical orientation at closest approach. In addition, because the increase on tether forces in the flexible system is greater than in the inclined maneuvers, the corresponding increase in tether mass is also larger. In the unmatched

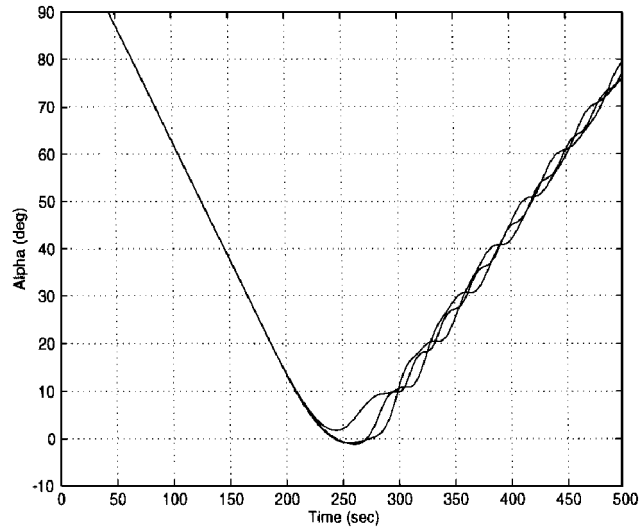

Fig. 17 Tether angles; flexible simulation of Jupiter flexible optimum, matched.

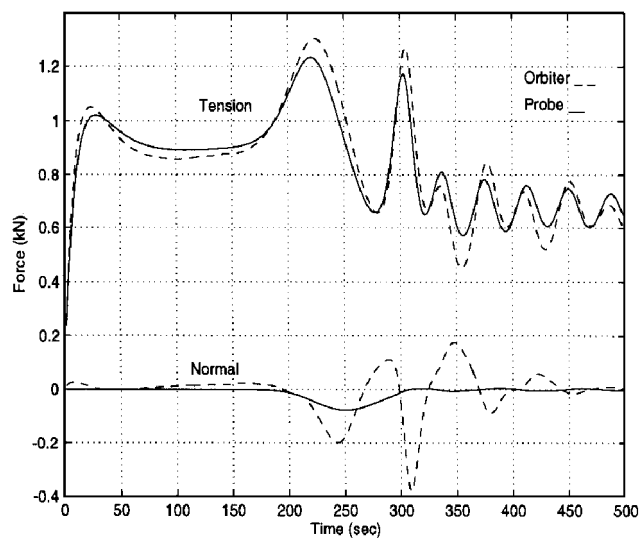

Fig. 18 Tether forces on the probe and the orbiter; flexible simulation of Jupiter flexible optimum, unmatched.

Table 2 Optimum maneuvers for flexible tether model (e_t = 0.9999, graphite tether)

Maneuver	Probe area, m^2	Δh_t, km	Length, km	Diameter, mm	Mass, kg	K_s, N/m	C, kg/s	$\dot{\alpha}_0$, rad/s	R_p, km
Mars (matched)	560	12.4	19.3	1.54	64.4	23.1	215	1.71*e*-2	3,484
Mars (unmatched)	100	12.4	18.7	1.53	62.1	23.7	217	1.66*e*-2	3,472
Jupiter (matched)	2,400	36.1	36.0	0.674	23.2	2.38	69.0	8.79*e*-3	71,877
Jupiter (unmatched)	500	36.1	38.9	0.680	25.5	2.24	66.9	7.68*e*-3	71,848

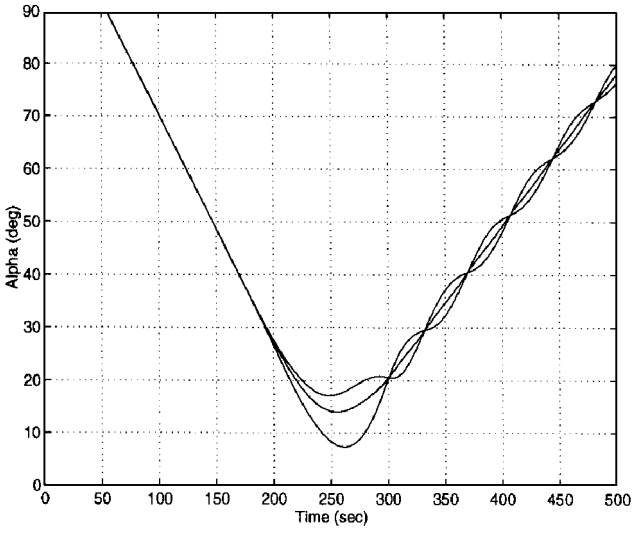

Fig. 19 Tether angles; flexible simulation of Jupiter flexible optimum, unmatched.

Jupiter maneuver, the changes due to tether flexibility are quite extreme (Figs. 18 and 19). The resulting optimum solution is much closer in behavior to an inclined maneuver, with the largest tension on the tether occurring at closest approach and a minimum orientation greater than zero. This change in the fundamental characteristics of the maneuver largely improves the behavior of the system. Bending is largely reduced, and the forces on the tether are much smaller. In addition, the normal forces on the orbiter also decrease. Using the flexible optimization, the increase in the tether mass in the unmatched system is only moderately larger than that found in the matched system. On the other hand, the flexible simulation of the optimum rigid solution predicts a very large change in tether mass associated with the large increase in tether forces. This clearly indicates that the rigid rod model fails to provide a good approximation of the optimum solution for the flexible tether in this case.

V. Conclusion

The flexibility effects on optimum maneuvers obtained using a rigid rod model can be significant. For inclined maneuvers, the rigid analysis provides a very good approximation to the flexible behavior. Given the computational demands associated with flexible tether analysis, the rigid tether model provides an invaluable tool in aerobraking tether analysis. On the other hand, the results in vertical dumbbell maneuvers are not very positive. Flexibility effects are significant, and, more important, the matching conditions, i.e., very large probe areas, must be satisfied for flexible vertical dumbbell maneuvers with reasonable tether mass. This indicates that the practical application of the vertical dumbbell maneuver may be limited. Note that in the unmatched case the optimum flexible solution is close to an inclined maneuver. This indicates that the inclined maneuver provides a much better solution to the tether aerobraking problem than the vertical dumbbell.

Nevertheless, the final conclusion is that the aerobraking maneuver remains feasible in a wide variety of conditions even when the analysis includes tether flexibility. In addition, in all cases analyzed here, the tether mass for the optimum flexible solutions remains much lower than the equivalent chemical propellant.

References

[1]Lorenzini, E., Grossi, M. D., and Cosmo, M., "Low Altitude Tethered Mars Probe," *Acta Astronautica*, Vol. 21, No. 1, 1990, pp. 1–12.

[2]Bergamaschi, S., and Bonon, F., "Equilibrium Configurations in a Tethered Atmospheric Mission," AAS/AIAA Astrodynamics Conf., AAS Paper 91-543, Durango, CO, Aug. 1991.

[3]Kirschke, M., Lorenzini, E., and Sabath, D., "A Hypersonic Parachute for Low-Temperature Reentry," 43rd IAF Congress, International Astronautical Federation, IAF Paper 92-0822, Washington, DC, Aug.–Sept. 1992.

[4]Keshmiri, M., and Misra, A. K., "Effects of Aerodynamic Lift on the Stability of Tethered Subsatellite Systems," AAS/AIAA Spaceflight Mechanics Meeting, AAS Paper 93-184, Pasadena, CA, Feb. 1993.

[5]Pasca, M., and Lorenzini, E. C., "Collection of Martian Atmospheric Dust with a Low Altitude Tethered Probe," AAS/AIAA Spaceflight Mechanics Meeting, AAS Paper 91-178, Houston, TX, Feb. 1991.

[6]Warnock, T. W., and Cochran, J. E., "Predicting the Orbital Lifetime of Tethered Satellite Systems," 43rd IAF Congress, International Astronautical Federation, IAF Paper 92-0002, Washington, DC, Aug.–Sept. 1992.

[7]Carroll, J. A., "Tether Applications in Space Transportation," *Acta Astronautica*, Vol. 13, No. 4, 1986, pp. 165–174.

[8]Puig-Suari, J., and Longuski, J. M., "Modeling and Analysis of Tethers in an Atmosphere," *Acta Astronautica*, Vol. 25, No. 11, 1991, pp. 679–686.

[9]Longuski, J. M., Puig-Suari, J., and Mechalas, J., "Aerobraking Tethers for the Exploration of the Solar System," *Acta Astronautica*, Vol. 35, No. 2/3, 1995, pp. 205–214.

[10]Longuski, J. M., Puig-Suari, J., Tsiotras, P., and Tragesser, S., "Optimal Mass of Aerobraking Tethers," *Acta Astronautica*, Vol. 35, No. 8, 1995, pp. 489–500.

[11]Tragesser, S. G., Longuski, J. M., Puig-Suari, J., and Mechalas, J. P., "Analysis of the Optimal Mass Problem for Aerobraking Tethers," AIAA Paper 94-3747, Aug. 1994.

[12]Puig-Suari, J., Longuski, J. M., and Tragesser, S. G., "Aerocapture with a Flexible Tether," *Journal of Guidance, Control, and Dynamics*, Vol. 18, No. 6, 1995, pp. 1305–1312.